



Nonisothermal crystallization kinetics: poly(ethylene terephthalate)–poly(ethylene oxide) segmented copolymer and poly(ethylene oxide) homopolymer

Xiaohua Kong^a, Xiaoniu Yang^a, Gao Li^{a,*}, Xiaoguang Zhao^a, Enle Zhou^a, Dezhu Ma^b

^a State Key Laboratory of Polymer Physics and Chemistry, Changchun Institute of Applied Chemistry, Chinese Academy of Sciences, Changchun 130022, People's Republic of China

^b Department of Materials Science and Engineering, University of Science and Technology of China, Hefei 230026, People's Republic of China

Received 11 April 2000; received in revised form 24 October 2000; accepted 2 March 2001

Abstract

The nonisothermal crystallization behavior of poly(ethylene oxide) (PEO) in poly(ethylene terephthalate)–poly(ethylene oxide) (PET–PEO) segmented copolymer and PEO homopolymer has been studied by means of differential scanning calorimetry, as well as transmission electron microscope. The kinetics of PEO in copolymer and PEO homopolymer under nonisothermal crystallization condition has been analyzed by Ozawa equation. The results show that Ozawa equation only describes the crystallization behavior of PEO-6000 homopolymer successfully, but fails to describe the whole crystallization process of PEO in copolymer because the secondary crystallization in the later stage could not be neglected. Due to the constraint of PET segments imposed on the PEO segments, a distinct two stage of crystallization of PEO in copolymer has been investigated by using Avrami equation modified by Jeziorny to deal with the nonisothermal crystallization data. In the case of PEO-6000 homopolymer, good linear relation for the whole crystallization process is obtained owing to the secondary crystallization does not occur under our experimental condition. © 2001 Elsevier Science Ltd. All rights reserved.

Keywords: Poly(ethylene terephthalate)–poly(ethylene oxide) copolymer; Poly(ethylene oxide) nonisothermal crystallization; Crystallization kinetics; Ozawa equation; Secondary crystallization

1. Introduction

Investigations of the kinetics of polymer crystallization are significant both theoretically and practically. Most frequently, the investigations are conducted under isothermal conditions because of the convenience of the theoretical treatment of the data. On the other hand, in practice, production and processing of the polymer are often carried out under nonisothermal conditions, typically the case of the melt spinning of fibers. There-

fore, the investigation of the kinetics of polymer crystallization under nonisothermal conditions is of great significance for the technological optimization and manufacture of high-performance polymeric materials. Some quantitative evaluations of the kinetics of nonisothermal crystallization have been reported [1–4]. However, because of the complication of the nonisothermal crystallization process, the different angle of consideration of the investigators and the different method of mathematical treatment, the applications of their theories are limited. From an experimental point of view, the technique of differential scanning calorimetry (DSC) is a frequently used method to study the nonisothermal crystallization temperature and enthalpy can

* Corresponding author. Fax: +86-431-5685653.
E-mail address: ydh@ns.ciac.jl.cn (G. Li).

be measured conveniently and quickly, and they are related to cooling rate.

Block copolymers are an interesting and already well-studied variation of polymers. In this class of polymer, it is possible to combine the properties of two completely different polymers without macroscopic phase separation occurring. Recently, block copolymer with crystallizing blocks have increasingly attracted the attention of scientists, because regulation of the crystal structure of the components offers an additional possibility of optimizing their properties [5]. However, less work has been reported on the nonisothermal crystallization kinetics of block copolymer, especially the block copolymer with two crystallizing blocks. In a previous work [6], we have studied the nonisothermal crystallization behavior of ethylene terephthalate–ethylene oxide segmented copolymers with two crystallizing segments. The results show that during the crystallization of the high- T_m segments (poly(ethylene terephthalate) (PET)), the low- T_m segments (poly(ethylene oxide) (PEO)) act as a non-crystalline diluent, the crystallization behavior of PET obeys Ozawa theory. When PEO segments begin to crystallize, the PET phase is always partially solidified and the presence of the spherulitic microstructure of PET profoundly influences the crystallization behavior, which result the overall crystallization process does not obey Ozawa equation.

This work presents the results of our investigation of the nonisothermal crystallization kinetics of PEO in PET–PEO segmented copolymer and PEO-6000 homopolymer by several kinetic approaches. The crystallization behavior of PEO-6000 homopolymer obeys Ozawa equation and Avrami equation modified by Jeziorny, while PEO in copolymer does not.

2. Experimental

2.1. Materials

The PET–PEO segmented copolymer was provided by the University of Science and Technology of China. The PEO segment has a weight-average molar mass, $\bar{M}_w = 6000$, the weight fraction of the PET segment in the PET30-PEO6 segmented copolymer is 0.30. PEO, with number-average molecular weight $\bar{M}_n = 6000$, was supplied by Shanghai Second Synthetic Detergent Firm.

2.2. Differential scanning calorimetry measurements

The nonisothermal crystallization process using a Perkin–Elmer DSC-7 under nitrogen purge by the following procedure. The samples (about 8 mg) of PET–PEO segmented copolymer and PEO-6000 homopolymer were heated to 280°C and 100°C, respectively and kept at this temperature for 3 min. They were then

cooled with different cooling rates (namely $R = 5, 10, 20, 40^\circ\text{C min}^{-1}$) and the heat flow during crystallization was recorded as a function of time. The relative crystallization, X_t , as a function of temperature is defined as:

$$X_t = \frac{\int_{T_0}^T (dH_c/dT) dT}{\int_{T_0}^{T_\infty} (dH_c/dT) dT} \quad (1)$$

where T_0 and T_∞ are the temperatures at which crystallization starts and ends, respectively.

2.3. Transmission electron microscope observations

A JEOL TEM 2010 EXII transmission electron microscope (TEM) was used to examine morphology at 200 kV. Droplets of 0.1 wt.% 1,1,2,2-tetrachloroethane solution of copolymer and 0.1 wt.% chloroform solution of PEO homopolymer were placed onto carbon-coated cleaved mica, respectively. First, the solvent evaporated at room temperature for about three days, the films then were held under vacuum at least 24 h. After post-annealing which was the same as those used for the DSC experiments (cooling rate is 5°C), pieces of the carbon and polymer film were next floated onto water and picked up with 400-mesh copper grids. Prior to observation by TEM, some of the specimens were exposed to vapors of hydrazine solution for 5 h, after the unsaturated bonds linked to the phenethyl of PET segments, they were then transferred and put under the vapors of an aqueous solution of osmium tetroxide (OsO_4) for 8 h. OsO_4 preferentially stains the unsaturated bonds of PET segments. The samples thus obtained were obliquely shadowed with Pt in a vacuum evaporator.

3. Theoretical background

Several methods for describing the crystallization kinetics are based on the Avrami equation [7]

$$1 - X_t = \exp(-kt^n) \quad (2)$$

where X_t is the relative degree of crystallinity; the exponent n is a mechanism constant whose value depends on the type of nucleation and growth dimension; the parameter k is a growth rate constant involving both nucleation and growth rate parameters.

Nakamura et al. [1,2] suggest a convenient procedure for using isothermal data for nonisothermal kinetics, on the basis of the following assumption: the rate of crystallization at time t only depends on the temperature and the relative crystallinity reached at that time, independently of the crystallization history.

Ozawa [4] extended the Avrami equation to the nonisothermal condition. Assuming that nonisothermal crystallization process may be composed of infinitesi-

mally small isothermal crystallization steps, the following equation has been derived:

$$1 - X_t = \exp(\varphi(T)/R^m) \quad (3)$$

where R is the cooling rate, X_t is the relative crystallinity at temperature T , $\varphi(T)$ is the cooling function of the process and m is the Ozawa exponent that depends on the dimension of crystal growth. According to the Ozawa analysis, if the relative crystallinities at different cooling rates at a given temperature are chosen, the plot of $\log[-\ln(1 - X_t)]$ versus $\log R$ should give a series of parallel lines. Then $\varphi(T)$ and m are determined from the intercept and slope, respectively.

One approach used in the literature to describe the nonisothermal crystallization process consists of applying the Avrami analysis to the data obtained from the nonisothermal crystallization thermograph [8–10]. During the nonisothermal crystallization process, the relation between crystallization time t and temperature T is given by:

$$t = \frac{|T_0 - T|}{R} \quad (4)$$

where T is the temperature at time t , T_0 is the initial temperature when crystallization begins ($t = 0$). Using Eq. (2) in double-logarithmic form, and plotting $\log[-\ln(1 - X_t)]$ against $\log t$ for each cooling rate, a straight line is obtained, from which values of the two adjustable parameters, k and n , can be obtained. It must be taken into account that in nonisothermal crystallization, the values of k and n do not have the same physical significant [9] as in the isothermal crystallization, due to the fact that under nonisothermal conditions the temperature changes constantly. This affects the rates of both nuclei formation and spherulite growth since they are temperature dependent. In this case, k and n are two adjustable parameters to be fit to the data. Although the physical meaning of k and n cannot be related in a simple way to the isothermal case, the use of Eq. (2) provides further insight into the kinetics of nonisothermal crystallization. Considering the nonisothermal character of the process investigated, Jeziorny [11] point out that the parameter for value of rate k should be adequately corrected. The factor that should be considered was the cooling rate R of the polymer. Assuming constant or approximately constant R the final form of the parameter characterizing the kinetics of nonisothermal crystallization (k_n) was given as follows:

$$\log k_n = \frac{\log k}{R} \quad (5)$$

While the Avrami and Ozawa equations were reasonable to some extent for many systems, a number of workers tried to use it to fit experimental results obtained from crystalline polymers and proposed some

modified form [12,13]. However, it is point out that all models currently available are inadequate in predicting nonisothermal crystallization kinetics based on isothermal data. For some polymer systems, such as poly(ether–ether–ketone) [9,10] and poly(ethylene oxide)/poly(methyl methacrylate) blends [14], their crystallization do not follow the Avrami and Ozawa equations.

4. Results and discussion

The results of the nonisothermal crystallization behavior of PET–PEO segmented copolymer and PEO-6000 homopolymer are shown in Fig. 1. The exothermic peak widens and shifts to lower temperature region as the cooling rate increases. The starting temperature (T_s), temperature (T_{max}) and time (t_{max}) at maximum heat flow (inflection point), and relative crystallinity X_{max} under different cooling rates of PEO in PET–PEO segmented copolymer and PEO-6000 homopolymer are listed in Table 1. The time to reach the inflection point increases with decreasing cooling rate. The maximum in the heat flow curves represents the changeover from the faster, primary process of crystallization to a slower, secondary process. This change results from the impingement of growing crystallites. Prior to impingement, crystals grow freely in a sea of amorphous polymer. After the impingement of adjacent crystals, further crystallization takes place in interlamellar regions and proceeds at a much slower rate. Similar conclusions about the existence of two-stage crystallization have been reached by Blundell et al. [15], and Lee and Porter [16]. For PEO in PET–PEO segmented copolymer, about 40% relative crystallinity has formed after time t_{max} for all cooling rates. This is in contrast to PEO-6000 homopolymer in which the relative degree of crystallinity at t_{max} increased with the increasing cooling rate, reaching a maximum of 60.6%. These qualitative observations indicate that nonisothermal crystallization kinetics of PEO in PET–PEO segmented copolymer are different from that of PEO-6000 homopolymer. This is reasonable as for PET–PEO segmented copolymer, when the copolymer is cooled from the amorphous phase to low temperature, PET segments crystallize first and proceed through free growth of spherulites from the homogeneous melt. The PEO segments act as a noncrystalline diluent during the crystallization of PET and start to crystallize later in the mixed region of PEO and amorphous PET.

Integration of the exothermic peaks during the nonisothermal crystallization process could give the relative crystallinity, X_t , as a function of temperature. The curves of relative crystallinity as a function of temperature are shown in Fig. 2 for PEO in copolymer (Fig. 2(a)) and PEO homopolymer (Fig. 2(b)). All curves in Fig. 2(a) show a reversed sigmoid shape, indicating fast primary

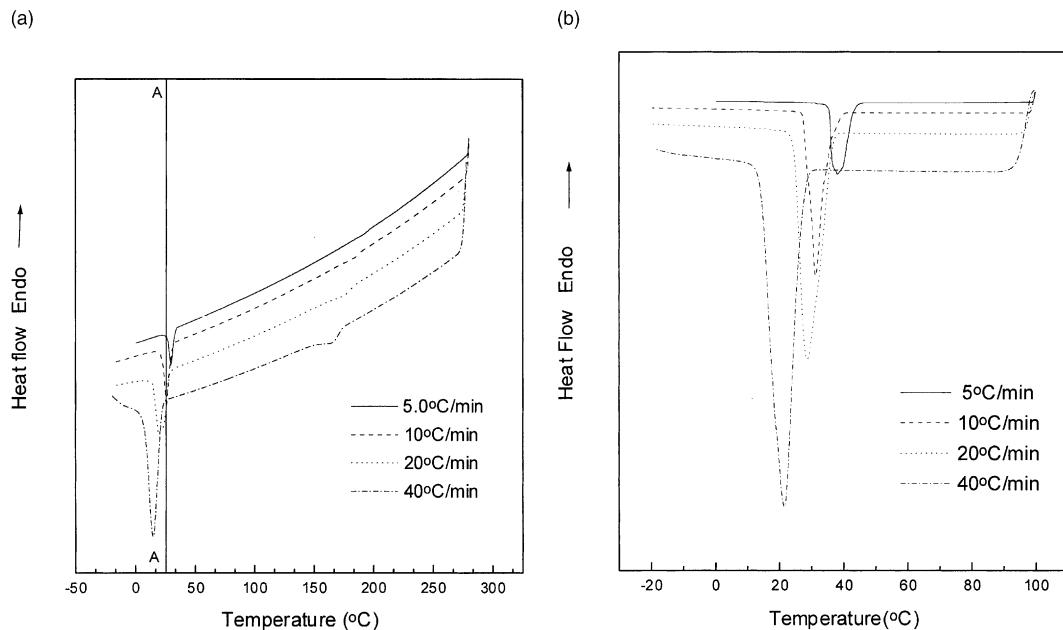


Fig. 1. DSC nonisothermal crystallization curves of (a) PET-PEO segmented copolymer and (b) PEO-6000 homopolymer at different cooling rates.

Table 1

Characteristic parameters of PEO in PET-PEO segmented copolymers and PEO-6000 homopolymer during nonisothermal crystallization process

Cooling rate (°C min ⁻¹)	PET-PEO				PEO-6000			
	T _s (°C)	T _{max} (°C)	t _{max} (min)	X _{max} (%)	T _s (°C)	T _{max} (°C)	t _{max} (min)	X _{max} (%)
5	41.6	30.7	2.17	44.4	47.8	38.2	1.91	44.2
10	39.5	28.7	0.98	42.3	42.2	31.2	1.10	50.5
20	35.1	24.7	0.52	44.1	40.1	28.6	0.58	56.3
40	32.0	18.8	0.33	41.4	32.0	21.4	0.27	60.6

crystallization during the early stages and slower secondary crystallization during the later stages. We observed that the crystallization develops rapidly, as if there were no nucleation processes and hence no induction period. This phenomenon is attributed to the crystallizability of PET in the PET-PEO segmented copolymer. To the contrary, Fig. 2(b) has a partial reversed sigmoid shape. The relative crystallinity still increases fast in the later portion on each curve. These indicate that PEO-6000 homopolymer has a significantly larger fraction of crystallization developing by primary processes.

Using Ozawa equation, the results of the nonisothermal crystallization kinetics of PEO in segmented copolymer and PEO-6000 homopolymer are shown in Fig. 3. From Fig. 3(a), it is evident that the Ozawa analysis does not adequately describe the nonisothermal

crystallization kinetics because a large portion of the crystallization is attributed to the secondary process. Generally, the crystallization of polymer consists of two processes: the primary crystallization and secondary crystallization followed. Ozawa assumed that the effects of secondary crystallization are negligible because it occurred in the later period and the temperature went down in the cooling crystallization process. Although it takes place in the later stage, the secondary crystallization is influenced greatly by the outside factors such as the cooling rate, and the effect could not be neglected for the nonisothermal crystallization of some polymer systems. Fig. 3(b), however, shows good linear relations, this indicates that the Ozawa analysis can be used to describe the nonisothermal crystallization of PEO-6000 homopolymer because secondary crystallization does not occur under our experimental condition.

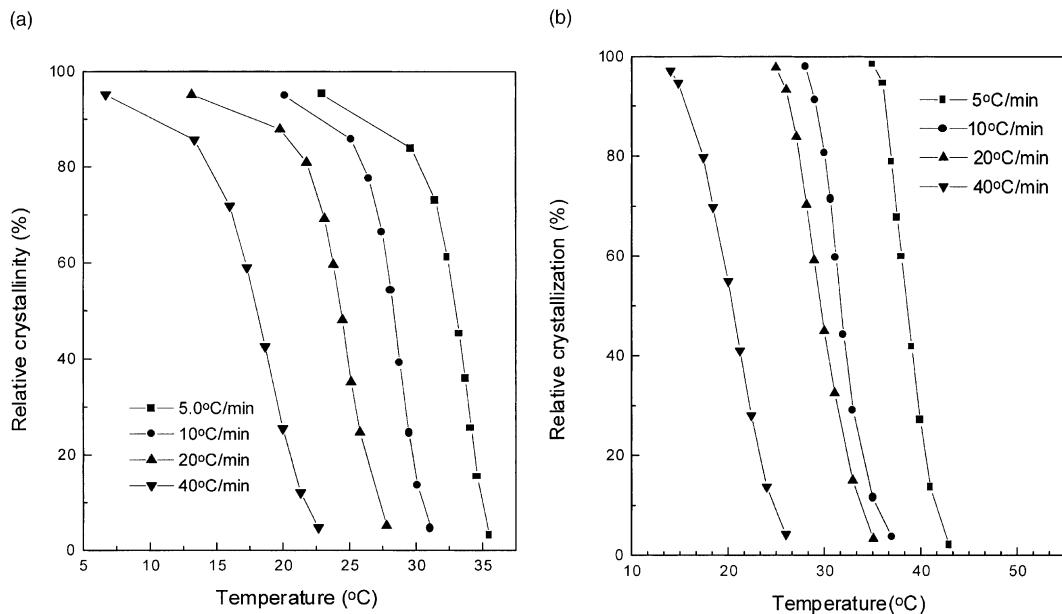


Fig. 2. Development of relative crystallinity with temperature for nonisothermal crystallization at the indicated rates of (a) PEO in PET-PEO segmented copolymer and (b) PEO-6000 homopolymer.

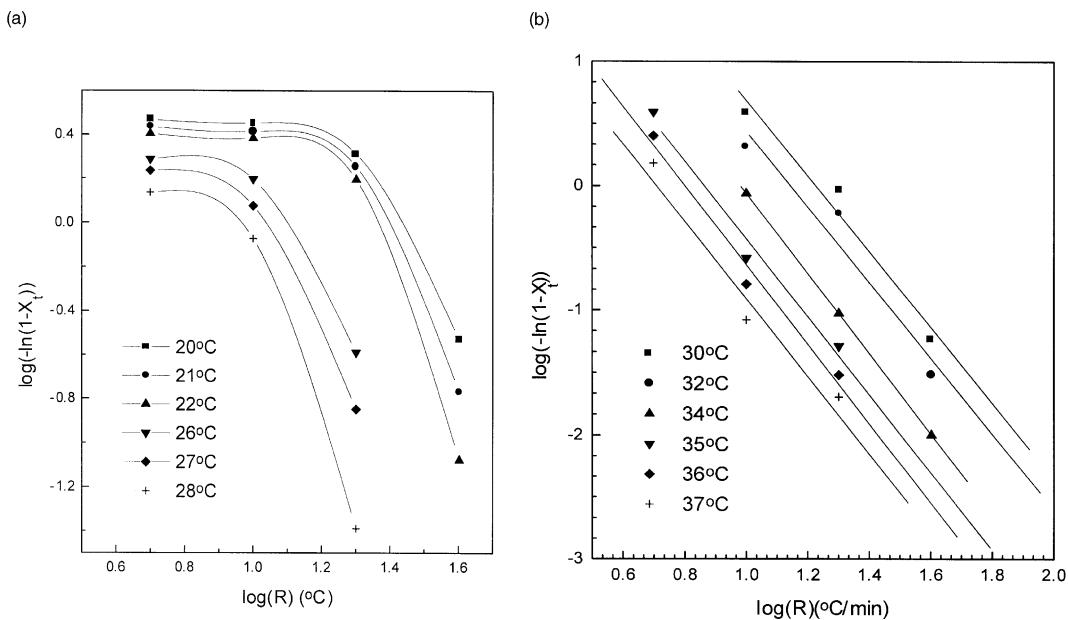


Fig. 3. Plots of $\log(-\ln(1-X_t))$ versus $\log R$ at the indicated temperature of (a) PEO in PET-PEO segmented copolymer and (b) PEO-6000 homopolymer.

Another reason for the failure of the Ozawa model may be due to the quasi-isothermal nature of the treatment. Referring to Fig. 1(a), the line AA represents the constant temperature 25°C. In the Ozawa analysis, the relative crystallinity is determined by the intersection of

the constant temperature line with the experimental data. Failure of the model may be attributed to the fact that the experimental data are obtained from widely varying physical states of the system. For the 25°C case, line AA intersects the $-40^\circ\text{C min}^{-1}$ data at the very

earliest stages of crystallization, and intersects the $-5^{\circ}\text{C min}^{-1}$ data when crystallization is nearly completed. The crystallization kinetics should be very different at low and high relative crystallinity, but the Ozawa analysis takes no account of these differences.

According to Eq. (4), the temperature scale could be transformed into time scale, then the relative crystallinity X_t as a function of time will be obtained. The Avrami plots according to Eq. (2), $\log[-\ln(1-X_t)]$ against $\log t$ for different cooling rates are shown in Fig. 4. It is obvious that the initial stage of crystallization follows the Avrami equation and holds in the region from the beginning of crystallization to the roll-off to a secondary process. The deviation of the Avrami plots is attributed to spherulite impingement, which indicated that there is a slow secondary crystallization continues long after its boundary is formed. As pointed out by Keith [17] and Kieth and Padden [18], spherulitic growth proceeds with the systematic exclusion of less crystallizable or noncrystallizable “impurities” which collected between the fibrils of the spherulite. The average values of Avrami exponent for primary crystallization is 4.5 for PEO in PET–PEO segmented copolymer (Table 2), which corresponds to the three-dimensional spherical growth and thermal nucleation in the initial stage of crystallization where the free spherulitic growth approximation is valid. The distinct drop in the Avrami exponent might suggest the possibility of a diffusion controlled one dimensional slow secondary crystallization of this excluded material continues and fills in the

holes developed in the crystal [19]. Therefore, secondary crystallization might correspond to the formation of a new and more perfect and stable lamellae as a result of the lamella-thickening effect. In the case of PEO-6000 homopolymer, the average value of Avrami exponent for the whole crystallization process is 4.6 because secondary crystallization of PEO does not occur under our experimental condition, which is in good agreement with that result obtained by using Ozawa equation.

Shown in Fig. 5 are TEM micrographs of PET–PEO segmented copolymer and PEO-6000 homopolymer with the same thermal history as those for nonisothermal crystallization kinetics study (cooling rate $5^{\circ}\text{C min}^{-1}$). Fig. 5(a) is the morphology of PET–PEO segmented copolymer which was stained by OsO₄, in which the morphology of PET (black spots) distributed in the lamellae of PEO is observed because OsO₄ preferentially stains the unsaturated bonds of PET, however, the detailed structure was lost owing to the stain of OsO₄. Fig. 5(b) shows the morphology of PEO-6000 homopolymer, which is a complete spherulitic texture with an “eye-like” morphology near the spherulitic center, which is found for most spherulites during crystallization. The different mechanism of PEO crystallization between copolymer and homopolymer is results from the different phase states of the system existing when PEO begins to crystallize. For PET–PEO segmented copolymer, crystallization of PEO takes place at temperature well below the crystallization temperature of PET, which means that the crystallized PET will always be partially

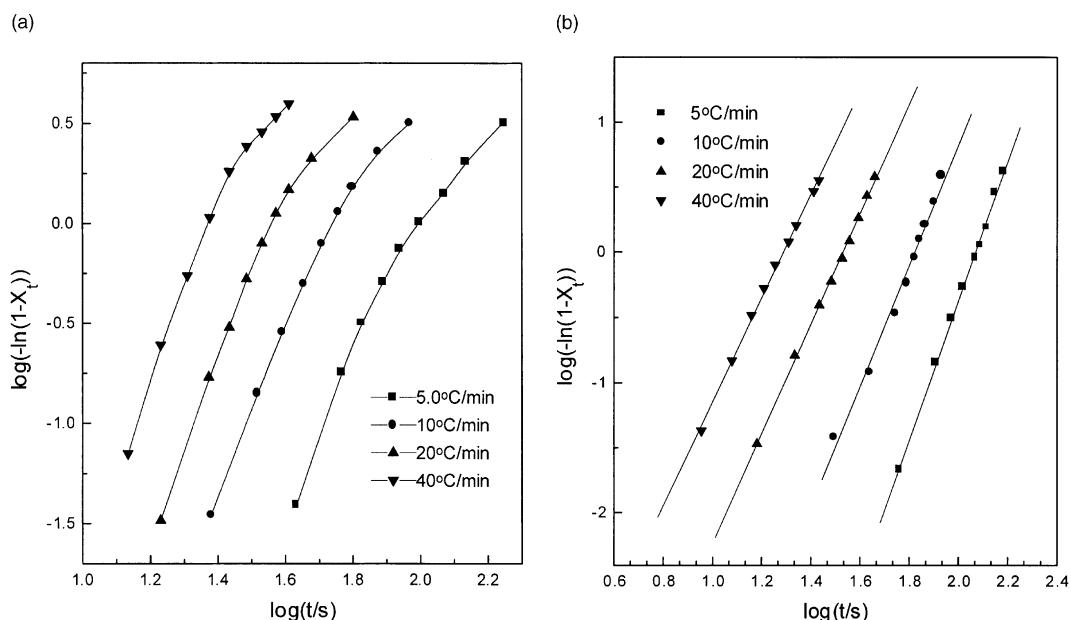
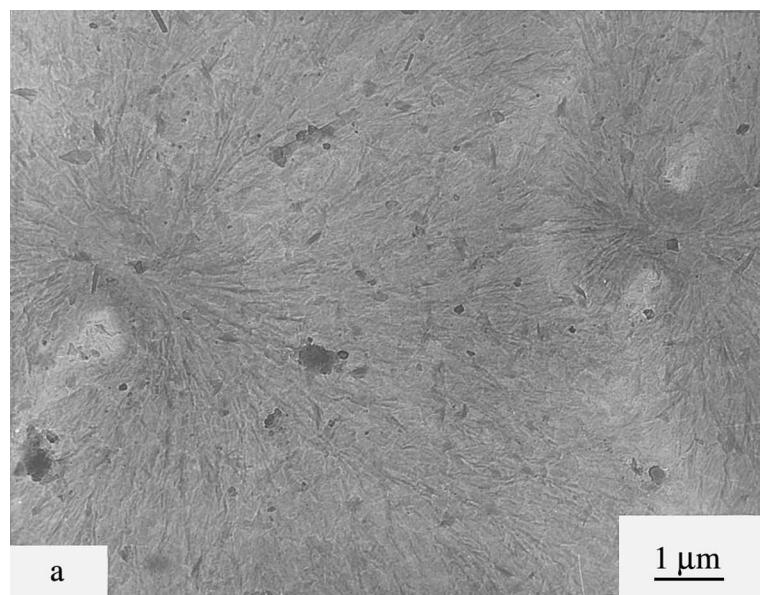


Fig. 4. Plots of $\log[-\ln(1-X_t)]$ versus $\log t$ of (a) PEO in PET–PEO segmented copolymer and (b) PEO-6000 homopolymer for nonisothermal crystallization at the indicated rate.

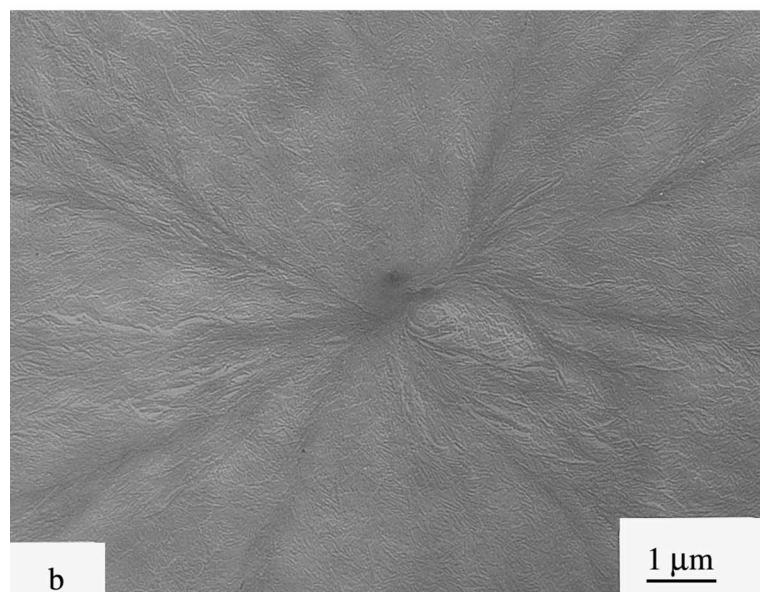
Table 2

Parameters n and $-\log k_n$ of PEO in PET–PEO segmented copolymers and PEO-6000 homopolymer from the Avrami analysis of nonisothermal crystallization

Cooling rate ($^{\circ}\text{C min}^{-1}$)	PET–PEO		PEO-6000	
	n	$-\log k_n$	n	$-\log k_n$
5	4.5	0.64	5.3	2.2
10	4.3	0.17	4.6	0.84
20	4.6	0.03	4.2	0.32
40	4.7	0.01	4.0	0.12



a

1 μm

b

1 μm

Fig. 5. TEM image of PET–PEO segmented copolymer after stained by (a) OsO_4 and (b) PEO-6000 homopolymer.

solidified when PEO starts to crystallize. The PEO segments, entangled with the PET chains, could only crystallize in their own domains and will be restricted by their own ability to undergo further crystallization, which results in slow secondary crystallization. However, crystallization of PEO homopolymer always occurs in a homogenous state, which results in a complete spherulitic structure shown in Fig. 5(b).

5. Conclusion

Nonisothermal crystallization kinetics of PEO in PET–PEO segmented copolymer and PEO-6000 homopolymer has been investigated by using DSC and TEM. The kinetics of PEO in copolymer and PEO-6000 homopolymer under nonisothermal crystallization condition has been analyzed by Ozawa equation. The crystallization behavior of PEO-6000 obeys Ozawa theory, while for PEO in copolymer, there is no agreement with Ozawa theoretical predictions in the whole crystallization process due to the secondary crystallization in the later stage could not be neglected. The crystallization mechanism and growth dimension of PEO in copolymer in the primary crystallization process are the same with those of PEO-6000 homopolymer. However, the crystallization behavior of PEO in copolymer appears to be strongly influenced by the presence of PET, which can be attributed to the fact that the PET phase is partially solidified at the temperatures where PEO crystallization takes place.

Acknowledgements

This work was supported by the National Key Projects for Fundamental Research, “Macromolecular

Condensed State”, of the State Science and Technology Commission of China, and the National Natural Science Foundation of China, and the Special Funds for Major State Research Projects. The authors are grateful to Prof. Dr. Stephen Z.D. Cheng for valuable discussions.

References

- [1] Nakamura K, Watanabe T, Katayama K, Amano T. *J Appl Polym Sci* 1972;17:1077.
- [2] Nakamura K, Katayama K, Amano T. *J Appl Polym Sci* 1973;17:1033.
- [3] Ziabicki A. *Coll Polym Sci* 1974;252:433.
- [4] Ozawa T. *Polymer* 1971;12:150.
- [5] Godovsky YuK, Yanul NA, Bessonsva NP. *Coll Polym Sci* 1991;269:901.
- [6] Kong XH, Yang XN, Zhou EL, Ma DZ. *Eur Polym J* 2000;36:1085.
- [7] Avrami MJ. *Chem Phys* 1939;7:1103.
- [8] Herrero CR, Acosta JL. *Polym J* 1994;26:786.
- [9] Cebe P. *Polym Compos* 1988;9:271.
- [10] Cebe P, Hong SD. *Polymer* 1986;27:1183.
- [11] Jeziorny A. *Polymer* 1978;19:1142.
- [12] Mandelkern L. *Crystallization of polymers*. New York: McGraw-Hill; 1964.
- [13] Wunderlich B. *Macromolecular physics*, vol. 2. New York: Academic Press; 1976.
- [14] Addonizio ML, Martuscelli E, Silvestre C. *Polymer* 1987;28:183.
- [15] Blundell DJ, Chalmers JM, Mackenie MW, Gaskin WF. *SAMPE Quarterly* 1986;17:1.
- [16] Lee Y, Porter RS. *Polym Eng Sci* 1986;26:633.
- [17] Keith HD, Padden FJ. *J Appl Phys* 1964;35:1270.
- [18] Keith HD. *J Polym Sci: Part A* 1964;2:4339.
- [19] Schultz JM, Scott RD. *J Polym Sci Part A* 1969;27:659.